

OMAE 005022

OFFSHORE VIV MONITORING AT SCHIEHALLION - ANALYSIS OF RISER VIV RESPONSE.

Stéphane F. A. Cornut

Deep Water Developments, BP Amoco
Exploration, Sunbury on Thames, UK

J. Kim Vandiver

Department of Ocean Engineering, MIT,
Cambridge, MA, USA

KEYWORDS

Vortex Induced Vibrations, Risers, Data Logging.

ABSTRACT

During November and December 96, a drilling riser in the Schiehallion field (West of Shetlands in 360m of water) was instrumented with accelerometers to record its Vortex-Induced Vibration (VIV) response in current. A paper has already been presented on the data gathering campaign (Hassanein, 1998). The present paper concentrates on the analysis of selected samples of the recording. This emphasis of the paper is twofold. The first is the investigation of the relationship between the shear of the velocity profile and the probability of single mode dominated response. The second is the determination of the reduced velocity bandwidth, ΔV_r , associated with the fluid excitation of the riser. Little is known about these quantities in the high Reynolds regimes found offshore. The first direct application of this work will be to better calibrate and further develop VIV prediction programs.

The results presented in this paper come from 83 samples of 28 minute long records. The raw accelerations were interpreted in terms of modal displacements (the normal modes were found from FE analysis). The current profile data are from acoustic Doppler current profile (ADCP) records that covered all but the top 60m of the water column.

INTRODUCTION

Risers, in large water depths and strong current environments, are prone to vibrations created by the vortices shed from the structure. These Vortex-Induced Vibrations (VIV) may damage the riser and limit its fatigue life. It is an important design consideration when drilling in high current environments.

Existing VIV prediction tools rely on empirical formulations based on the expected Strouhal number and reduced velocity bandwidth. The reduced velocity bandwidth is defined as that range of reduced velocity along the riser, which would result in synchronization of the vortex shedding process with the motion of the riser at a particular riser natural frequency. In other words, it is the approximate range of reduced velocity that could produce lock-in, and is the range of reduced velocity that defines the power-in region for each mode of interest. In present day practice, the expected values of these parameters are usually based on laboratory experiments conducted at subcritical Reynolds numbers. However, for Reynolds numbers above 10^5 , there is little experimental data on long flexible cylinders such as drilling risers. To overcome this lack of experimental data a month-long offshore monitoring campaign was conducted.

The objective of the data analysis was to use the full-scale VIV data to better understand single and multiple mode response behavior and to obtain best fit estimates of the reduced velocity bandwidth for modes observed in the response data. These results are then to be used in to improve VIV response prediction tools.

DESCRIPTION OF THE RISER AND THE DATA GATHERING SYSTEM

A riser on the Paul B. Loyd rig, drilling in the Schiehallion Field, West of Shetland in 360m of water, was instrumented with accelerometers. In parallel, the current was monitored with an Acoustic Doppler Current Profiler (ADCP), giving a precise description of current velocities through the water column. The data gathering campaign lasted for about 21 days. A more detailed description of the full logging system is given in Hassanein (1998). The riser length from the flex joint at the bottom to the ball joint at the top was 368m. The average mass per unit length in the buoyant portion of the riser was 770kg/m,

and the diameter of the buoyant sections was 1.124m. The riser had buoyancy from water level to bottom. The non-buoyant section was 0.533m (21 inches) in diameter and had an average mass per unit length including contents of approximately 570kg/m. Typical top and bottom tensions varied from 3100kN (700kips) to 2800kN.

Current

The Acoustic Doppler Current Profiler (ADCP) gave recordings of current speed every 16m in the water column. The velocity is calculated as an average of the recordings over 10min. The averaging process smoothes out the effects of the semi-submersible motions and thruster noise.

The current was measured from 60m to 300m below the water surface. Readings at the surface and on the bottom of the sea bed are not possible with the ADCP because of reflections from the rig structure, the sea surface, and the sea bed.

Riser Vibrations

The VIV was recorded with three Robit DACOS data loggers. These worked as independent units fixed on the riser. They measured and recorded internally the horizontal acceleration of the riser (2 accelerometers in X and Y directions) at a rate of 5Hz for 27minutes every 48minutes. When the riser was pulled out of the water, the units were recovered, and the information was transferred onto a PC for processing.

The riser was equipped with three DACOS data loggers. The loggers were positioned at the anti-nodes of the first five modes of vibration. These modes were the most important contributors to the riser response during the measurement period. Table 1 and Figure 1 show the position of the data loggers.

Table 1. Data logger positions, for Riser length L = 368m.

	Height above the Lower Flex Joint: Z	Ratio to Riser Length: Z/L	Located at anti-nodes for modes
DACOS 1	46m	~L/8	4
DACOS 2	88m	~L/4	2
DACOS 3	186m	~L/2	1, 3, 5

DATA PROCESSING

Preliminary analysis of the data showed that VIV modes 1 to 4 were present and that the maximum current speed went up to 0.75 m/s (1.5 knots). From the more than 600, 28 minute long samples, 83 were identified for further analysis. These were selected to provide a representative range of VIV conditions – high to low mode numbers, single and multi mode response, high and low current velocities, and a range of current shear.

One purpose of this study was to extract estimates of the reduced velocity bandwidths from the current and riser response

data. To do this it was necessary to make assumptions about the relationship between riser response and current profiles. These included the assumption that the dominant VIV response is transverse to the current direction, and that the excitation of the riser for any particular mode occurs in a region where the vortex shedding frequency is close to the natural frequency of that mode. To simplify the interpretation of the data, some data sets were rejected due to excessive directional variation over the water column or excessively non-monotonic behavior. Others were excluded because of significant data contamination due to surface wave action. 83 samples were used in the final analysis.

Although some cases were excluded because they were too complex, it is the authors intention to first develop an understanding of the response to the simpler current profiles. Once a methodology has been proven to work for the simpler cases, then the more complex ones may be considered. A pragmatic step by step approach is being taken.

Processing of current data

The current velocity was extrapolated from –60m to the surface. The current at the sea bed was assumed to be 0.0m/s, allowing interpolation between the bottom and the lowest measured point. Three 10 minute-averaged ADCP records were averaged to correspond to the 28 minute acceleration records.

Processing of Riser Accelerations

The recorded transverse riser acceleration was contaminated with gravitational components due to rotation of the riser with respect to the vertical. In order to get around this problem, a simplified method was used to estimate modal displacements. First, preliminary examination of the data revealed that the dominant responding modes were the first three transverse bending modes. Modes one and three have anti-nodes near the mid-point of the riser, L/2. Mode two has an anti-node near L/4 and at 3L/4. At the anti-node of a particular mode the local tilt due to rotation is zero, resulting in no gravitational contamination at that point. Therefore, modal displacements for modes one and three were estimated directly from the acceleration records at L/2 and modal displacements for mode two were estimated from the recordings at L/4. Mode 4 was never dominant, but when present could be estimated from the logger at L/8, the anti-node for mode four.

To further assist in the estimation of the modal displacements, the acceleration signals were band-pass filtered around the natural frequency of the mode of interest and then double integrated.

DATA ANALYSIS

The recorded data showed that the riser was exposed to current up to 0.75m/s (1.5 knots), exciting a VIV response up to mode 4. The drilling riser was almost buoyant with a low mass ratio ($m/\rho.D^2=0.90$). The Reynolds numbers recorded were

frequently above 10^5 , providing information about VIV for a flow regime rarely reached during laboratory experiments.

In the analysis to follow the average modal response is estimated from the entire 28 minute record. However, it will be shown that substantial fluctuation in the modal response occurred when more than one mode participated in the response. The natural frequencies of modes also vary from sample to sample. This is due to changes in top tension, mud weight, drill string tension and added mass distribution. In the analysis to follow, the reported reduced velocity is computed with the actual observed natural frequency, and not with a single fixed value of the natural frequencies of the riser. Thus the effects of variation of natural frequency are included in the reduced velocities as reported in this paper. One consequence of this, is that when one plots modal response A/D versus reduced velocity, the range of reduced velocity corresponding to lock-in is confined to a narrower range of reduced velocities.

The first part of the response data analysis focuses on the identification of single mode and multi-mode response. The results are compared to a simple prediction reported by Vandiver et al. (1996), which is based on the value of the shear fraction and the number of potentially excited modes.

The second part of the data analysis provides estimates of the reduced velocity bandwidth that best characterize the response of this drilling riser.

SINGLE AND MULTI MODE RESPONSE

When predicting the VIV response of a riser, it is important to determine whether a single mode will dominate, resulting in lock-in, or whether several modes respond together in a multi-mode response. Single mode lock-in normally results in larger response amplitudes and shorter fatigue life, and it is therefore important to develop the capability to predict each type of behavior on the basis of the expected current profiles and the riser structural properties. Vandiver et al. (1996) revealed an apparent relationship between the probability of occurrence of single-mode dominance, the Shear parameter, β , and the number of potentially responding modes, N_s . This hypothesis was based on observations from laboratory experiments conducted by Shell (Allen, 1994). Data from the Schiehallion field experiments are tested against the response model derived from the Shell data.

The Shear parameter is a measure of the spatial variation of the current along the water depth. It is defined as follows: $\beta = \Delta V / V_{av} = (V_{max} - V_{min}) / V_{av}$, where V_{max} , V_{min} , V_{ave} are respectively the current profile maximum, minimum and average velocities. The average value is a spatial average over the water column. The number of potentially responding modes is obtained as follows.

The highest potentially excited frequency will be given by:

$$f_{high} = \frac{V_{max}}{V_{rmin} \cdot D} \text{ where } D \text{ is the diameter of the riser and}$$

V_{rmin} is the lower bound of the reduced velocity bandwidth (A value of 4.0 is used in first approximation).

The number of potentially responding modes (N_s) is found by dividing f_{high} by the frequency of the first mode (f_1):

$$N_s = \frac{V_{max}}{V_{Rmin} \cdot D \cdot f_1}$$

Figure 2 shows the Shear parameter, $\beta = \Delta V / V_{av}$, on the x axis and the number of potentially responding modes, N_s , on the y axis. Vandiver, Allen and Li (1996) presented a similar plot of data from flexible cylinders in sheared flow at sub-critical Reynolds numbers. Their data revealed that the N_s versus β curve could be divided into two regions, corresponding to single or multi-mode dominated response behavior. The boundary between the two regions was described in probabilistic terms. As one moved across the boundary between the two regions, the probability of single mode response grew or diminished depending on the direction. This boundary is shown in Figure 2 as two straight line segments. Single mode behavior is more likely below the horizontal line and to the right of the near vertical line segment, while multi-mode response is more likely above the horizontal line and to the left of the near vertical segment.

The response for each of the 83 cases is plotted with different symbols indicating single mode response, two modes responding, or three modes responding. The following criterion was applied to the measured data to determine if a mode was active or not. The response spectrum was computed and divided up into bands, one for each of the first five modes of vibration. The area or integral through each peak in the spectrum is a measure of the power or energy of vibration associated with each particular mode. A mode was considered active if the modal power associated with its spectral peak was greater than 10% of the power corresponding to the maximum modal power peak in the spectrum. This simple criterion, when applied to the Schiehallion data, resulted in the statistics given in Table 2. The horizontal line dividing Region I from II is taken from Vandiver et al. (1996). Above the line, Region I is expected to be more likely to experience multi-mode behavior. Below the line in Region II single mode behavior is expected to be more likely. This is consistent with the data shown here.

Vandiver et al. (1996) also suggested that at shear parameter values greater than about 1.4, it was likely that single mode dominance would be expected even with reasonably large values of N_s , the number of potentially responding modes. Unfortunately, this full scale data set had insufficient data with a shear fraction in excess of 1.4, so it was impossible to determine whether or not this predicted phenomenon actually occurs at super-critical Reynolds numbers.

Table 2. Single and multi-mode response statistics as a function of the number of potentially responding modes for shear fraction between 0.5 and 1.3

	Single mode	Multi mode
Region I ($N_s > 3$)	8	15
Region II ($N_s \leq 3$)	34	26

Region I is the multi-mode region.

Region II is the single mode, low N_s region ($N_s \leq 3$) and includes all points for which $N_s = 3$.

On the whole, the data has similar trends as the Shell experiment (Allen, 1994). For higher N_s , the likelihood of the response being multi-mode increases. However, as in the Shell experiments, there does not seem to be a clear boundary between the type of responses. Indeed, quite a large number of multi-mode responses is present in region II and some single mode responses appear in region I.

The explanation could lie in the fact that the time of monitoring for one sample (28 minutes) is very long. It is thus possible that different single mode responses occurred in succession, and were interpreted as a multi-mode response. To investigate this possibility, three samples have been selected and their time series have been analyzed. Samples 32, 46 and 76, all present cases which by the simple 10% criteria based on the energy in a peak, were interpreted as multi-mode response combining modes 1 and 2. For each the number of potentially responding modes was 2 and the shear fraction was respectively 1.07, 0.80 and 0.62.

The modal amplitudes of mode 1 and 2 have been extracted. Figure 3 shows the results for sample 46. The top part is X_1^2 (corresponding roughly to the envelope of the square of the modal amplitude of mode 1), the bottom part is $-X_2^2$. Similar plots for samples 76 and 32 are presented in Figures 4 and 5.

Each of the plots shows a different balance of power between the modes. Sample 76 shows a dominant mode 1, frequently joined by response of mode 2. Much of the time the response is multi-moded. Sample 46 in Figure 3 has comparable levels of response for modes 1 and 2. At times they exist together and sometimes they appear only one at a time. This record exhibits both single and multi-mode response depending on the moment. Sample 32 in Figure 5 shows a dominant mode 2, occasionally yielding to mode 1 dominance. Most of the time single modes are dominant.

These three examples all came from Region II where single mode dominance according to Vandiver et al. (1996), is more likely to occur. As shown in the examples, single mode dominance does occur, but precise prediction of when it occurs and how long it lasts remains an unresolved problem. It is certain that the details of the velocity profiles are important. For completeness the three current profiles corresponding to these examples are plotted in Figure 6.

This set of measurements extends the results of the Shell laboratory experiments as presented in Vandiver et al. (1996) to high Reynolds number and more realistic slenderness ratios.

ESTIMATION OF THE REDUCED VELOCITY RANGE OF THE MODAL POWER-IN ZONES

This section presents estimates of the reduced velocity band which best accounts for the observed riser vibrations. The first problem, to be overcome, is that measurements of the vortex shedding frequency along the riser do not exist. The only measurements are of the current profile and the riser response. The reduced velocity limits of the power-in region for each mode must be deduced from the current profiles and the measured response. The principal problem is that even though it is known that a particular mode had significant response, the region on the riser with lift forces at the same frequency as the natural frequency is not known. Two approaches have been taken. In the first, it has been assumed that the average current speed corresponds to the predominant vibration frequency. This is equivalent to assuming that the current is nearly uniform. This method is expected to give reasonable answers for low sheared profiles. With the exception of the uniform flow case this method is very biased and will tend to underestimate both the upper and lower bounds of the reduced velocity range. The bias will become more severe with increases in the shear of the velocity profile.

In the second approach, the maximum current speed in the profile is assumed to correspond to the vibration frequency of the highest responding mode. This second approach has the advantage of not being dependent on the degree of shear of the current profile. However, this method is also biased and will tend to overestimate the reduced velocity associated with the response of any specific mode.

Neither method is guaranteed to give the correct answer, but the two methods do bound the correct answer. Estimates based on the average velocity tend to underestimate the value of the reduced velocity whereas estimates based on the maximum velocity overestimate the reduced velocity.

Method 1: $V_R = V_{ave}/(f_{dom} \cdot D)$. As mentioned before, this approach is strictly correct for cases where the shear fraction is equal to zero (uniform current). For sheared flows the method will tend to underestimate the reduced velocity. Indeed, it is assumed that the mode responding at f_{dom} is excited by the velocity V_{ave} , whereas the predominant mode is more likely to be excited by a higher velocity than the average velocity.

The reduced velocity for Method 1 is defined in the following way: $V_R = V_{ave}/(f_{dom} \cdot D)$. Widely accepted sub-critical Reynolds number laboratory data would suggest that the power-in zone for a particular mode on a riser would have upper and lower reduced velocity limits of approximately 4 to 8. Full scale drilling risers operate at higher Reynolds numbers. The values of the reduced velocity, V_{Rmax} and V_{Rmin} , which define the

power-in regions are not well known. The data from the Schiehallion riser gives some useful insight.

Figure 7 is a plot of reduced velocity versus shear fraction. The reduced velocity is based on the average current speed and the frequency of the dominant peak in the spectrum. The various symbols indicate which mode was associated with the dominant peak. Small shear fraction means the profile is close to uniform, and the observed reduced velocities will not be too biased. When the shear fraction, β , is less than 0.75 means that the current speed varied less than 38% above or below the average current. These cases are enclosed in a box in Figure 7. For all cases in the box the dominant responding mode was the first mode. This data suggests that the range of reduced velocities, which correspond to first mode dominance, is in the range of 3.7 to 6.6. However, because the reduced velocity was computed based on the average velocity this range of values is likely to be lower than actual.

An alternative way to plot the data in Figure 7 is shown in Figure 8, which shows a plot of reduced velocity versus Reynolds number ($Re = V_{ave} \cdot D / \nu$). Four different symbols indicate the amount of the shear fraction, β . The data falls into four groups, each with a different slope. Each group corresponds to a dominant response frequency, which is assumed to be one of the first four natural frequencies

In Figure 8, four lines can be fitted to the data, corresponding to each dominant mode. The slope of each line can be estimated by $\frac{v}{f_{dom} \cdot D^2}$ since $V_R = v \cdot Re / (f_{dom} \cdot D^2)$, and v is the kinematic viscosity ($1.3 \cdot 10^{-6} \text{ m}^2/\text{s}$). The measurements line up reasonably well. The scatter comes from variation of the response frequency f_{dom} , due to variations in added mass, and in the tension of the riser and drill string. Table 3 gives the slope corresponding to each mode.

This figure reveals that most of the data is dominated by first and second mode events. The points corresponding to first mode lie on the line furthest to the left. The second mode points are next to it with third and fourth mode following in order. An average estimate of the natural frequency for each of the modes can also be extracted from these lines by eliminating the diameter and the viscosity. These estimates are shown in the second row of Table 3.

Table 3. Line slopes from Figure 8. One line for each mode, 1 to 4.

	Mode 1	Mode 2	Mode 3	Mode 4
Slope ($v/f_{dom} \cdot D^2$)	1.78×10^{-5}	8.91×10^{-6}	6.53×10^{-6}	4.54×10^{-6}
f_{dom}	0.057 Hz	0.114 Hz	0.156 Hz	0.224 Hz

Method 2: $V_R = V_{max} / (f_{max} \cdot D)$. The first method gave values which are expected to be too low. A different approach is now used, which will overestimate the reduced velocity

range. The maximum velocity of the current profile, V_{max} , and the frequency of the highest responding mode, f_{max} is used to compute the reduced velocity. This should result in an overestimate of the Reduced Velocity, because it is assumed that the velocity corresponding to the highest observed frequency is the maximum velocity on the riser.

Figure 9 shows how the variation of V_{max} may or may not be well correlated with vibration frequency of the highest responding mode f_{max} .

Let's assume (Case 1), that V_{max} corresponds to a reduced velocity slightly larger than V_{Rmin} for mode N. The power in region of mode N is starting to develop at the top of the riser where mode N-1 is still predominant. As V_{max} increases (Case 2), the mode N power-in region grows in size. When V_{max} reaches a value corresponding to a reduced velocity above V_{Rmax} , the power in region stops growing and a power-in region for mode N+1 starts appearing (case 3).

By identifying the range of velocity between case 1 and case 3, it is possible to characterize the reduced velocity bandwidth for mode N. If in Case 3 the reduced velocity for mode N were computed using V_{max} , the resulting value would be higher than the actual maximum value of the reduced velocity for mode N.

Figure 10 has been plotted showing the reduced velocity ($V_R = V_{max} / (f_{max} \cdot D)$) as a function of the Reynolds number ($Re = V_{max} \cdot D / \nu$), classified by highest responding modes. Highest responding mode means the mode with the highest natural frequency, which appeared in the response spectrum. It does not mean that it was the dominant mode. Again the data falls into groups through which straight lines have been drawn. Each of these groups corresponds to the highest responding mode. The first at the left side of the curve is for those cases that had only first mode response. The next group to the right had mode 2 as the highest responding mode, but includes many cases with both mode 1 and 2 responding. The third and fourth groups had modes 3 and 4 as the highest responding modes. The slope of each line is given by $v / (f_{max} \cdot D^2)$ since $V_{max} = v \cdot Re / (f_{max} \cdot D^2)$.

Some interesting observations can be made from this graph. First, relying on the concepts illustrated in Figure 9, one can infer the upper and lower reduced velocities for some of the modes, based on the following interpretive rules:

Rule 1: The lowest reduced velocity at which a mode first appears is an approximation of V_{Rmin} for that mode (Case 1, Mode N, Figure 9).

Rule 2: The V_{max} at which mode N first appears, is the value which corresponds to V_{Rmax} for mode N-1 (Also Case 1, Mode N-1, Figure 9).

Applying these rules leads us to the following conclusions:

- Mode 2 starts appearing at a reduced velocity of about 3.5. thus, $V_{Rmin}^{(2)} \sim 3.5$
- Mode 1 has a reduced velocity of approximately 7.0 when mode two first appears. Therefore, $V_{Rmax}^{(1)} \sim 7.0$
- Mode 3 first appears with a reduced velocity of 4.5. Therefore, $V_{Rmin}^{(3)} \sim 4.5$
- Mode 2 has a reduced velocity of approximately 6.5 when mode three first appears. Therefore, $V_{Rmax}^{(2)} \sim 6.5$
- Mode 4 has only 4 data points and the lowest begins before any of the mode three points. This is not fully understood. It may be excitation from in-line forces at twice the lift force frequency or it may be due to some other excitation.
- From the first appearance of mode 2 to the first appearance of mode three spans a reduced velocity range of 3.5 to 6.5.
- From the earlier analysis by method 1, the reduced velocity range deduced from the low shear mode one data, suggested a range of 3.7 to 6.7. From 1 above $V_{Rmax}^{(1)} \sim 7.0$

The conclusion of the above analysis is that the reduced velocity range defining the power-in regions for this riser are approximately given by: $3.5 \leq V_R \leq 6.5$

The mean value or center of this range is $V_{Rmean} = 5.0$. An approximate Strouhal number corresponding to the center of the reduced velocity bandwidth is given by:

$$St = 1/V_{Rmean} = 0.2.$$

RESPONSE RMS-A/D AS A FUNCTION OF REDUCED VELOCITY

Figure 11 shows the modal response ($Rms A^{(2)}/D$) of the riser for mode 2 only as a function of reduced velocity defined as ($V_{R}^{(2)} = V_{max}/f_2 \cdot D$). The different symbols show which mode was dominant at the time. Data points for which Mode 1 was dominant lay to the left hand side of the graph, have low, mode 2, reduced velocity and have small mode two response. Similarly, Mode 3 and 4 dominated cases are to the right hand side, have low mode 2 response, but have high, mode 2, reduced velocities. The peak A/D response for mode two occurs at a $V_{Rmax}^{(1)} \sim 7.5$, which the authors believe corresponds to a condition such as that shown in Case 3 of Figure 9, with $N = 2$. That is to say, for mode 2 to have maximum response in a sheared flow, it must have a fully developed power-in region, spanning the entire possible range of reduced velocity for mode 2. The actual reduced velocity corresponding to the top of the power-in range would frequently coincide with velocities somewhat less than V_{max} . Figure 11 suggests that an upper bound for the upper limit of the power-in reduced velocity range is 7.5. The earlier estimate of the upper limit estimate based on the data in Figure 10 was 6.5.

As with Figure 10, Figure 11 reveals considerable overlap in the occurrence of dominant modes. For V_R between 4 and 6, mode 1 conflicts with mode 2. For V_R between 6.5 and 9, mode 2 conflicts with mode 3. Yet single mode dominance does occur as discussed earlier in the paper.

Figure 12 shows the curve giving the best statistical fit through the data presented in Figure 11. One can see some resemblance to the typical response curve from uniform flow laboratory data. However, because of the shear flow, it must be interpreted slightly differently. The reduced velocity for which mode 2 starts to appear can be identified. If the threshold level is defined for the initiation of mode 2 response as $Rms A^{(2)}/D > 0.1$, then the corresponding lower limit reduced velocity is given as, $V_{Rmin}^{(2)} \sim 3.5$. As explained above, the upper reduced velocity limit corresponds to the largest mode 2 power in region on the riser. In Figure 12, the maximum $Rms A^{(2)}/D$ response occurs when $V_{Rmax}^{(2)} \sim 7.5$.

CONCLUSIONS AND RECOMMENDATIONS

This study derives important parameters for the understanding and modelling of risers subject to VIV. The results are based on full-scale drilling riser data. Conditions are more realistic than experiments carried out in laboratories - high Reynolds numbers, sheared currents and multi-mode response are typical of the data being considered.

The first finding concerns the characterization of the riser response with respect to multi-mode or single mode domination. It is shown that the trend found by Vandiver et al. (1996) is generally verified. However, the boundaries are fairly loose. The possibility of having multi-mode response, even for cases where the potential number of excited mode is low, should not be discarded. Single mode dominated cases do also occur. Insufficient data was available to comment on the probability of occurrence at shear fractions greater than 1.4. More work remains to be done with this data set to determine the probability of occurrence of single mode versus multi-mode response.

Useful estimates were obtained for the reduced velocity limits, which define the power-in regions of individual modes at Reynolds numbers up to one million. Table 4, below, summarizes the findings and relates them to the method used and to the modal information used.

Table 4. Reduced Velocity Band Estimates from Three Methods.

Method	Mode Number	V_{Rmin}	V_{Rmax}	$St = 1/V_{Rmean}$
$V_{ave} \& f_{dom}$	1	3.7	6.7	0.19
$V_{max} \& f_{max}$	2	3.5	6.5	0.20
$V_{max} \& f_{max}$	3	4.5	-	-
$V_{max} \& A/D$	2	3.5	7.5	0.18

It has been shown that the lower reduced velocity limit of the power-in zone is approximately 3.5 and the upper limit is between 6.5 and 7.5. The Strouhal Number, defined as the inverse of the mean reduced velocity in the power-in band is approximately 0.19 to 0.20. It should also be noted that despite a fairly short riser, with relatively widely separated natural frequencies, considerable overlap in modal dominance has been observed.

ACKNOWLEDGMENTS

The authors wish to thank Christophe Legros and Thanos Moros for their help and support during the analysis the riser VIV data and the writing of this paper.

REFERENCES

Allen D., Dension E, Bos J, 1994, "Vortex Induced Vibration of Cylindrical Structures in Sheared Flow", Data Reports 1-7, Shell E&P Tech Co., Houston, Texas.

Hassanein T., Fairhurst P., 1998, "Challenges in the Mechanical and Hydraulic Aspects of Riser Design for Deep Water Developments", IBC Offshore Pipeline Technology Conference, Oslo.

Vandiver K., Li L, 1997, "Shear 7: Theory Manual", MIT.

Vandiver K., Allen D., Li L., 1996, "The Occurrence of Lock-In under Highly Sheared Conditions", Journal of Fluids and Structures, Vol. 10, pp.555-561.

Vandiver K., 1993, "Dimensionless Parameters Important to the Prediction of Vortex Induced Vibration of Long Flexible Cylinders in Ocean Currents", Journal of Fluids and Structures, Vol. 7, pp.423-455

Figure 1: Position of the accelerometers along the riser of length L.

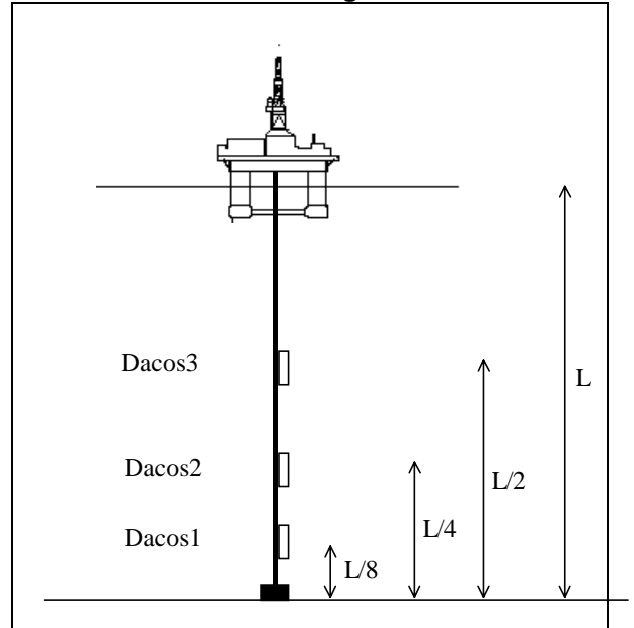


Figure2: Number of Potentially Responding Modes vs. Shear Fraction.

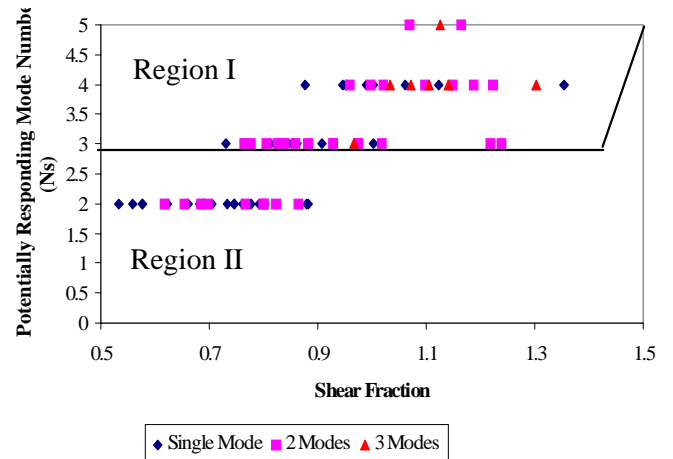


Figure 3: Sample 46, Modal Displacement Envelope of Mode 1 (top) and Mode 2 (bottom).

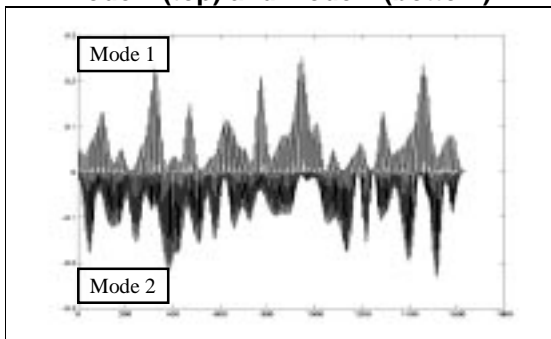


Figure 4: Sample 76, Modal Displacement Envelope of Mode 1 (top) and Mode 2 (bottom).

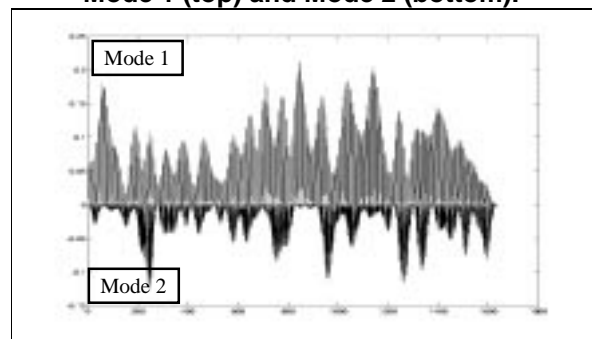


Figure 5: Sample 32, Modal Displacement Envelope of Mode 1 (top) and Mode 2 (bottom).

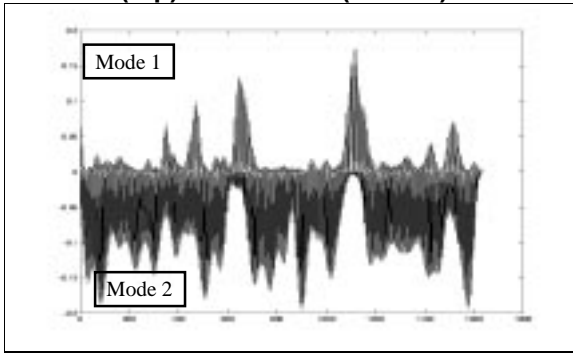


Figure 7: Reduced Velocity (average) vs. Shear Fraction.

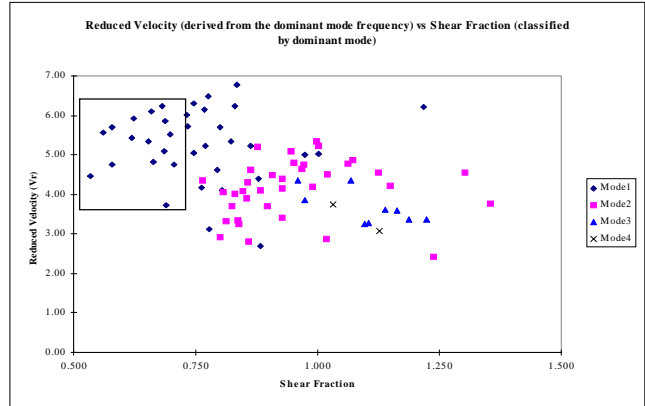


Figure 6: Current Velocity Profiles for Samples 32, 46 and 76.

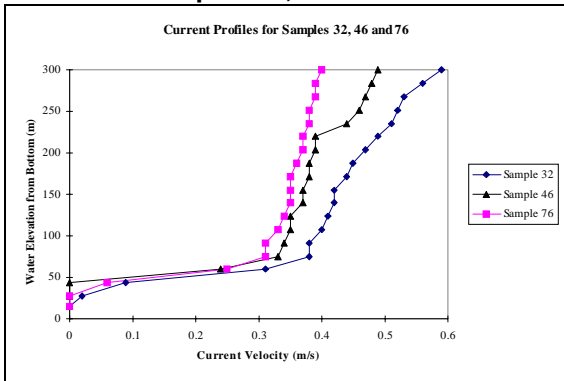


Figure 9: VIV Power Region Lay out as a function of V_{max}

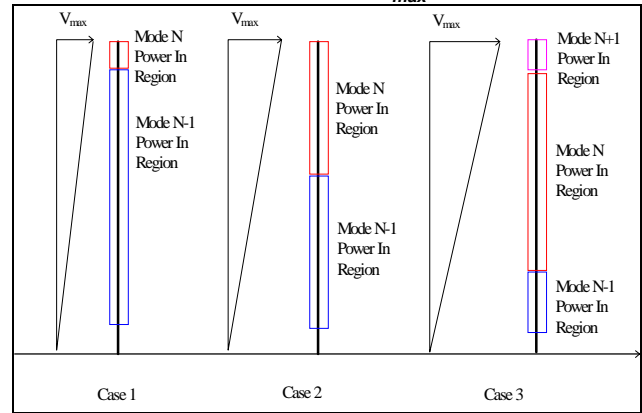


Figure 8: Reduced Velocity (average) vs. Reynolds Number (average) (by Shear fraction group).

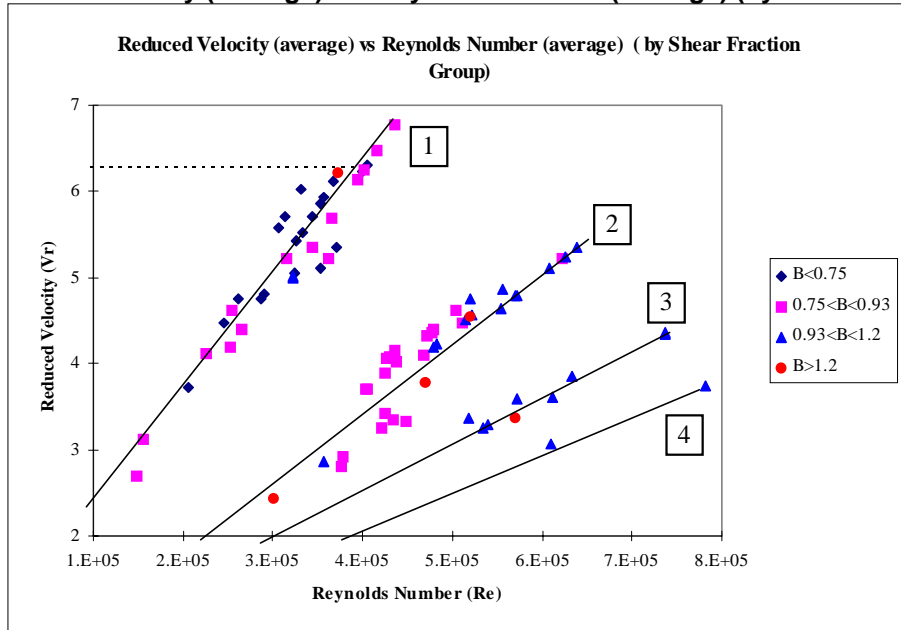


Figure 10: Reduced Velocity (max) vs. Reynolds Number (max) (by highest responding mode).

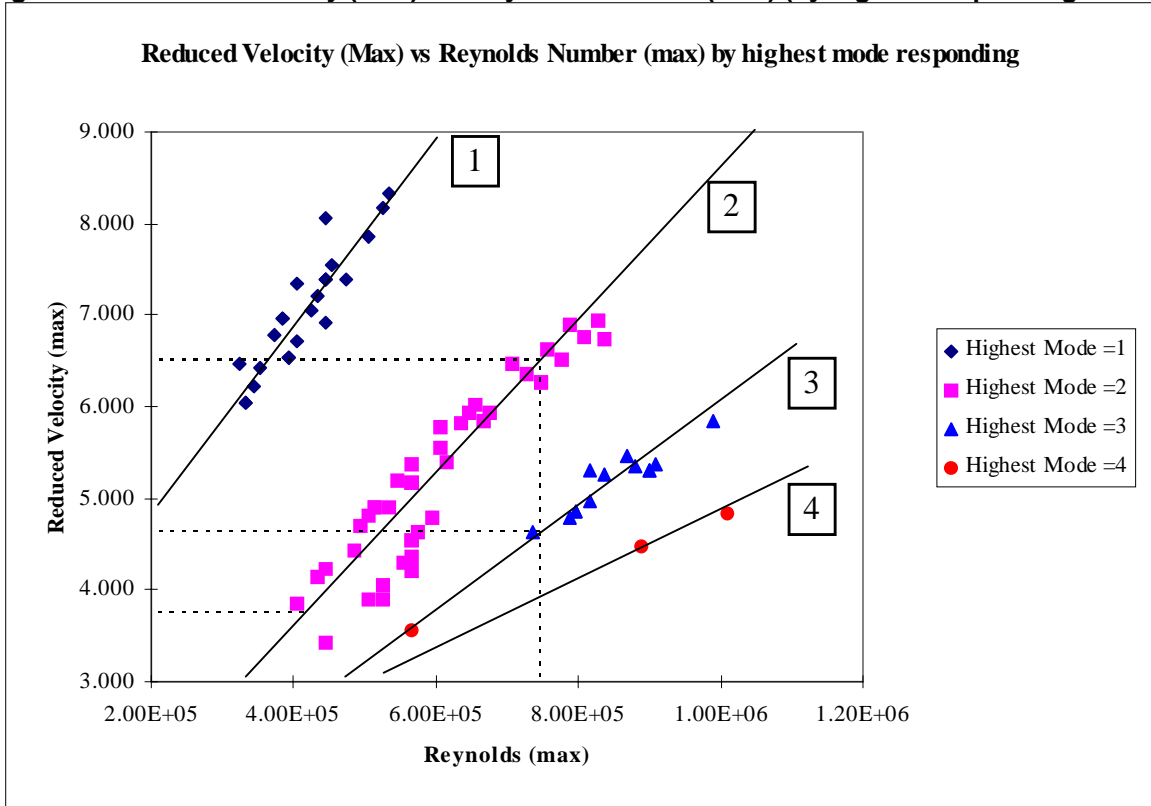


Figure 11: RMS A/D vs. Reduced Velocity (max) for Mode 2 (by predominant mode).

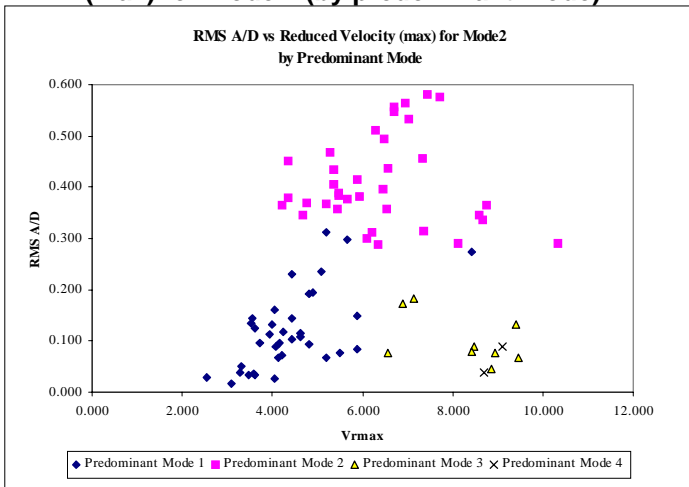


Figure 12: RMS A/D vs. Reduced Velocity (max) for Mode 2.

